

2

-----TATION PAGE

Form Approved  
OMB No. 0704-0188

AD-A241 989



d to average 1 hour per response, including the time for reviewing instructions, searching existing data sources, reviewing the collection of information. Send comments regarding this burden estimate or any other aspect of this burden, to Washington Headquarters Services, Directorate for Information Operations and Reports, 1215 Jefferson Avenue, Washington, DC 20503.

T DATE

1991

3. REPORT TYPE AND DATES COVERED

Final

4. TITLE AND SUBTITLE

Some simple design considerations for binary optical holographic elements

5. FUNDING NUMBERS

6. AUTHOR(S)

Jerome B. Franck  
Van A. Hodgkin

DTIC  
SELECTED  
C D

7. PERFORMING ORGANIZATION NAME(S) AND ADDRESS(ES)

Wester Space and Missile Center  
Engineering Directorate  
Vandenberg AFB, CA 93437-6021

8. PERFORMING ORGANIZATION REPORT NUMBER

WSMC-TR-91-03

Naval Weapons Center  
China Lake CA 93555

9. SPONSORING/MONITORING AGENCY NAME(S) AND ADDRESS(ES)

10. SPONSORING/MONITORING AGENCY REPORT NUMBER

11. SUPPLEMENTARY NOTES

12a. DISTRIBUTION/AVAILABILITY STATEMENT

Approved for public release; distribution is unlimited

12b. DISTRIBUTION CODE

Distribution Statement  
A

13. ABSTRACT (Maximum 200 words)

It has been shown previously that an optical analysis based on a ray trace can prove to be beneficial in the design of binary type phase holograms, because the optical path of each ray must be taken into account. Binary elements converted directly from thick, classically designs to Fresnel/binary equivalents, without a redesign will probably have reduced performance. Furthermore, the phase prescription developed by sophisticated lens design programs may not be manufacturable. Some simple design examples are presented to illustrate natural and manufacturing constraints.

91-14051



91 10 24 081

14. SUBJECT TERMS

Optical analysis, Holography, Holograms, Ray tracing, Fresnel lens Gratings, Optical Lens, Optical Phenomena, Binary Optics

15. NUMBER OF PAGES

9

16. PRICE CODE

17. SECURITY CLASSIFICATION OF REPORT

unclassified

18. SECURITY CLASSIFICATION OF THIS PAGE

unclassified

19. SECURITY CLASSIFICATION OF ABSTRACT

unclassified

20. LIMITATION OF ABSTRACT

SAR

## GENERAL INSTRUCTIONS FOR COMPLETING SF 298

The Report Documentation Page (RDP) is used in announcing and cataloging reports. It is important that this information be consistent with the rest of the report, particularly the cover and title page. Instructions for filling in each block of the form follow. It is important to *stay within the lines* to meet optical scanning requirements.

### Block 1. Agency Use Only (Leave blank).

**Block 2. Report Date.** Full publication date including day, month, and year, if available (e.g. 1 Jan 88). Must cite at least the year.

**Block 3. Type of Report and Dates Covered.** State whether report is interim, final, etc. If applicable, enter inclusive report dates (e.g. 10 Jun 87 - 30 Jun 88).

**Block 4. Title and Subtitle.** A title is taken from the part of the report that provides the most meaningful and complete information. When a report is prepared in more than one volume, repeat the primary title, add volume number, and include subtitle for the specific volume. On classified documents enter the title classification in parentheses

**Block 5. Funding Numbers.** To include contract and grant numbers; may include program element number(s), project number(s), task number(s), and work unit number(s). Use the following labels

C	Contract	PR	- Project
G	Grant	TA	- Task
PE	Program Element	WU	- Work Unit
			Accession No

**Block 6. Author(s)** Name(s) of person(s) responsible for writing the report, performing the research, or credited with the content of the report. If editor or compiler, this should follow the name(s)

**Block 7. Performing Organization Name(s) and Address(es)** Self explanatory

**Block 8. Performing Organization Report Number** Enter the unique alphanumeric report number(s) assigned by the organization performing the report

**Block 9. Sponsoring/Monitoring Agency Name(s) and Address(es)** Self-explanatory

**Block 10. Sponsoring/Monitoring Agency Report Number** (If known)

**Block 11. Supplementary Notes** Enter information not included elsewhere such as: Prepared in cooperation with , Trans of , To be published in . When a report is revised, include a statement whether the new report supersedes or supplements the older report

**Block 12a. Distribution/Availability Statement.** Denotes public availability or limitations. Cite any availability to the public. Enter additional limitations or special markings in all capitals (e.g. NOFORN, REL, ITAR)

DOD - See DoDD 5230.24, "Distribution Statements on Technical Documents."

DOE - See authorities.

NASA - See Handbook NHB 2200.2.

NTIS - Leave blank.

### Block 12b. Distribution Code.

DOD - Leave blank

DOE - Enter DOE distribution categories from the Standard Distribution for Unclassified Scientific and Technical Reports.

NASA - Leave blank

NTIS - Leave blank

**Block 13. Abstract.** Include a brief (*Maximum 200 words*) factual summary of the most significant information contained in the report

**Block 14. Subject Terms** Keywords or phrases identifying major subjects in the report.

**Block 15. Number of Pages** Enter the total number of pages

**Block 16. Price Code** Enter appropriate price code (*NTIS only*)

**Blocks 17. - 19. Security Classifications** Self-explanatory. Enter U S Security Classification in accordance with U S Security Regulations (i.e., UNCLASSIFIED). If form contains classified information, stamp classification on the top and bottom of the page

**Block 20. Limitation of Abstract** This block must be completed to assign a limitation to the abstract. Enter either UL (unlimited) or SAR (same as report). An entry in this block is necessary if the abstract is to be limited. If blank, the abstract is assumed to be unlimited



Accession For	
NTIS ORAD	<input checked="" type="checkbox"/>
DTIC TAB	<input type="checkbox"/>
Unannounced	<input type="checkbox"/>
Justification	
By	
Distribution/	
Availability Codes	
Dist	Special
A-1	

## Some simple design considerations for binary optical holographic elements

Jerome B. Franck

Western Space and Missile Center/Engineering  
Vandenberg Air Force Base, Ca 93437-6021

Van A. Hodgkin

Naval Weapons Center  
China Lake, Ca 93555

### ABSTRACT

It has been shown previously<sup>1-4</sup> that an optical analysis based on a ray trace can prove to be beneficial in the design of binary type phase holograms, because the optical path of each ray must be taken into account. Binary elements converted directly from thick, classically designs to Fresnel/binary equivalents, without a redesign will probably have reduced performance. Furthermore, the phase prescription developed by sophisticated lens design programs may not be manufacturable. Some simple design examples are presented to illustrate natural and manufacturing constraints.

### 2. INTRODUCTION

Current advances in microlithographically produced holographic optical phase elements, sometimes called binary optics (BO), have presented the optical engineer with a powerful tool for solving design problems. While previous workers<sup>1-4</sup> have presented careful, mathematically rigorous analysis, the design engineer may find it difficult to interpret the results with respect to potential pitfalls. With BO element production costs still quite high, it would be no laughing matter to discover that the optical design program that was supposed to design a positive BO lens had not been properly set up and while the program's display showed the proper ray trace for a positive lens, it had actually designed a negative lens! Without an independent check to verify the software developed design, the optical engineer might not find out that a problem exists until the element, at a cost of \$25k, is delivered and tested.

The above scenario is a real possibility with the complexity of the optical design software today. The error could be compounded further by either an incorrect optical prescription or a prescription that current microlithographic technology is incapable of producing. It is beyond the scope of this paper to address the problems associated with the lens design software pitfalls mentioned previously. Rather, some simple design examples will be presented to act as a tutorial. The first example will briefly illustrate a basic error of assumption. It shows the importance of performing a ray trace on the element under design. The second example will illustrate a more fundamental problem in manufacturability and will address the efficiency of one of the simplest optical elements possible: a binary approximation of a Fresnel type wedge or prism. The purpose of this example is to provide, by analogy, a feel for the efficiency of a BO element.

### 3. BACKGROUND

BO holographic elements may be thought of as step-wise, i.e. quantized, approximations of continuous phase structures. The purpose of these phase structures is to modify the optical wavefronts propagating through a region to achieve a desired wavefront. To begin with, we look at a standard thick lens as shown in Fig. 1a. Incoming light from an on axis point source at infinity reaches the lens. In transition through the element the continuously varying thickness (optical path length) of the lens introduces a corresponding phase change in the transmitted wavefront. An analogous optical structure is the Fresnel equivalent of the same lens as shown in Fig. 1b. The important criterion here is that the radial regions, or Fresnel zones, shown in cross section have much the same curvature as the thick lens with the main difference being that from the base of one zone to the peak of the adjacent zone the light must be in phase. More will be said about this constraint later. Each optical section may be characterized by a vertical edge, i.e. a discontinuity.

and a continuously varying thickness that introduces a phase change in the transmitted wavefront. A BO would have as a difference a step-wise approximation of this continuous surface. Obviously, quite a bit may be learned by studying the Fresnel lens since it represents the BO limiting case where the number of steps goes to infinity and the surface changes from step-wise to continuous. The efficiency of the BO can therefore be no better than that of the Fresnel lens. The number of steps used are a consequence of the number of masking and etching processes. As the number of steps increase the optical efficiency of the element will increase towards the value for the Fresnel equivalent of the thick lens. The discontinuity and angularly induced shading will add to a loss of efficiency compared to the thick lens. The thick lens, assuming a well manufactured surface, will have a loss due to the Fresnel reflections from the front and back surface. This same reflective loss for BO's is often mentioned and passed over in discussions on BO element efficiency information. Since much of the developmental BO work is being performed in the infrared (IR), and IR materials may have quite high indices of refraction, the reflective losses at the surface may be quite high (approaching 40%). Unlike a thick lens which may be anti-reflective coated to reduce reflection losses to a few percent, coating BO may be fraught with problems. Multilayer relief structures may suffer from waveguiding that could have disastrous effects and have been shown to produce spurious spatial orders with some orders exhibiting a high degree of efficiency<sup>5</sup>.

#### 4. DESIGN EXAMPLE (1)

In the first design example, a comparison is made between a thick lens and its Fresnel equivalent as shown in Fig. 1a and Fig. 1b respectively. The comparison here has been discussed previously<sup>1-4</sup>, but is important enough to be restated in a slightly different manner. Fig. 1a shows a thick lens producing the image of a point object that is located on axis at infinity, and, ignoring diffraction, four rays traversing the system are shown to image to a point. (In the case of a spherical surface, the curved surface should be placed in the front rather than the rear in order to produce minimum spherical aberration.) The addition of an aspheric component, assumed here, can greatly reduce the spherical aberration to acceptable levels. Shown in Fig. 1b is the same surface prescription, but with the curved surface collapsed to produce the Fresnel equivalent. For the thick lens, the edge ray 1a intersects the optical axis at point  $p_1$  as does the ray 2a from the central zone. However, the same situation is not true for the Fresnel equivalent shown in Fig. 1b. While the edge ray 1b, like its counterpart ray 1a, is unchanged by the flattening of the lens and thus intersects the optical axis at  $p_1$ , ray 2b leaves the rear surface at the same angle as 2a, but the rear surface has been collapsed closer to the front surface. This introduces an optical path difference (OPD) between ray 2b and ray 2a, which can be seen by the fact that ray 2b intersects the optical axis at  $p_2$  that is back along the optical axis from  $p_1$  a distance equal to the thickness change of the central section.

There is of course a focal shift at each Fresnel zone. However, unlike normal third order spherical aberration, there is no focal shift within a given zone. These focal shift errors are quantized in nature. The focal shift between zones is a function of both the thickness change, which is a result of collapsing the thick lens, and the separation between the zones which is not constant.

#### 5. DESIGN EXAMPLE (2)

The next example is a simple optical element that will be designed and analyzed in some detail. The results should prove illustrative in showing that it is not always possible to have complete control of a design situation due to fundamental restraints.

There are several approaches that may be taken to determine the performance of a design. While a rigorous vector theory approach would provide the most accurate results, a scalar approach should provide some insight. Even here, there are several paths that may be taken. For this example it will be assumed that diffraction is the critical phenomena and refraction effects are secondary. Conditions for diffraction will be assumed and Snell's Law will then be invoked under these constraints, and while small angles are assumed, larger angles will be used here for illustration. An approach utilizing Fourier analysis similar to Goodman<sup>6</sup> will be discussed later.

Perhaps the simplest optical element next to a planar window is a wedge or prism. Its properties are well known and the analysis required to convert the element to a Fresnel equivalent and then a BO are easy to follow and provides

insight that is not obscured by complex geometry. Also, a cautious analogy may be drawn between the bending of a ray by a region of the BO wedge and a region of a lens.

The first portion of the analysis will concern itself with converting a thick wedge to a Fresnel wedge. Shown in Fig. 2 is a thick, right triangular wedge of refractive index  $n_1$  and wedge angle  $\alpha_1$ . For simplicity, light enters the back surface at normal incidence angle and is incident on the rear surface at angle  $\alpha_1$ . If the surrounding media has an index of refraction  $n_2$ , the light exits the rear at angle  $\alpha_2$  according to Snell's Law given by

$$n_1 \sin(\alpha_1) = n_2 \sin(\alpha_2), \quad (1)$$

Now, we wish to produce Fresnel equivalent of the thick wedge, as shown in Fig. 3. This is essentially a grating structure whose properties are given by the standard grating equation

$$d \sin(\theta_m) = m \lambda, \quad (2)$$

where  $d$  is the grating period,  $m$  is the grating order and  $\lambda$  is the wavelength of the illuminating light. We will assume that we are given a required angle  $\theta$  for the light exiting the grating. The efficiency will be a maximum when each Fresnel wedge has the same exiting angle  $\theta$ , from Fig. 2 it can be seen that

$$\alpha_2 = \alpha_1 + \Theta, \quad (3)$$

Substituting Eq (3) into Eq (1) gives

$$n_1 \sin(\alpha_1) = n_1 \sin(\alpha_1 + \Theta), \quad (4)$$

or, with a bit of trigonometric manipulation

$$\tan(\alpha_1) = \sin(\Theta) / n \cos(\Theta), \quad (5)$$

where  $n = n_1/n_2$ .

Now, returning to Fig. 3, we want the number of light waves in the grating media with index of refraction  $n_1$  to differ by an integral number of waves in the external media with index of refraction  $n_2$  (taken here to be air) directly adjacent to the vertical section. This condition is obtained if the height of the sawtoothed step is given by

$$h = q \lambda / (n_1 - 1) \quad (6)$$

where  $q$  is an integer. Then for the right triangle of Fig. 2

$$\tan(\alpha_1) = h / d = q \lambda / [d(n_1 - 1)], \quad (7)$$

where  $d$  is both the base of the right triangle and the grating period. Equating  $\tan(\alpha_1)$  in Eqs (5) & (7) and solving for  $d$ , we get

$$d = \frac{q \lambda [n \cos(\Theta)]}{(n_1 - 1) \sin(\Theta)} \quad (8)$$

We have found the dimensions for the right triangular subprisms for the Fresnel wedge that satisfies both Snell's Law and the grating equation for a given output angle, wavelength and index of refraction. However, with these constraints can we also expect high efficiency for the directed light? To get a feel for the answer we solve Eq (2) and Eq (8) for

the order number, which is usually assumed to be an integer, and we find that

$$m = \frac{q[n - \cos(\Theta)]}{(n_1 - 1)} \quad (9)$$

Clearly, we are not free to pick  $m$ . It is constrained by the output angle  $\Theta$  that was specified and the available refractive index. We can choose the "best" index available, but at visible wavelengths we are limited at present by the materials that have been developed for use as BO elements. We have some leeway by being able to choose  $q$  for the optimal  $m$ , but we must remember that  $q$  appears in Eq. (8) also. In the IR, the situation is even worse because the number of IR transmitting materials is limited to a few candidates. Shown in Fig. 4 is a plot of  $m$  versus exitance angle  $\Theta$  for several indices of refraction for the integer  $q = 1$ .

By designing a Fresnel wedge with available materials we can get a feel for the imposed constraints and the ramifications towards performance. Two designs will be demonstrated utilizing the same material at two extreme wavelengths:  $10 \mu\text{m}$  in the IR and  $0.35 \mu\text{m}$  in the ultraviolet (UV), with the same design angle of exitance  $\Theta$ . These wavelengths severely limit the choice of available materials. Therefore NaCl will be used because its index of refraction of approximately 1.5 is nearly constant, even though it has actually had little or no developmental work as a BO material. An exit angle of  $20^\circ$ , is chosen as a reasonable design constraint.

Given  $n_1 = 1.5$ ,  $\Theta = 20^\circ$ ,  $n_2 = 1$ , and  $\lambda = 10 \mu\text{m}$  and a  $q = 1$  by solving Eq (6) for the height of one of the subprisms shown in Fig. 3 we get  $h = 20 \mu\text{m}$ . The wavelength of the light in the NaCl is medium is given by  $\lambda_{\text{NaCl}} = \lambda/n_1$  and is  $6.66 \mu\text{m}$ .

From Fig. 5, we see that we have been successful in matching the phase of the light exiting the top portion of a subprism and the light at an adjacent point that has traveled in air, i.e. there are exactly three waves in the NaCl and two waves in the air. Next, we calculate the grating period  $d$ , and hence the base of each subprism, from Eq (8) and find that  $d \approx 32.8 \mu\text{m}$ , and we find that  $m = 1.13$  from Eq(9). Now, to convert the Fresnel wedge to a BO equivalent, we remember that the number of levels, i.e. steps,  $N$  is related to the number of masks and etch procedures  $M$  by

$$N = 2^M \quad (10)$$

which is why the term binary is used. (For example, if  $M = 1$  then  $N = 2$ , if  $M = 2$ , then  $N = 4$ , if  $M = 3$ , then  $N = 8$  and so on and so forth.) Current technology currently supports up to a four mask process for several materials. So, for this design we will assume a four mask process that will therefore produce 16 steps. The width of each step is  $w = d/N$ , so for this example with  $d \approx 32.8 \mu\text{m}$  and  $N = 16$   $w \approx 2.0 \mu\text{m}$ . The height of each binary step  $h = h/N$ , and with values we've chosen  $h \approx 1.25 \mu\text{m}$ . Both  $h$  and  $w$  thus calculated are well within the range of current microlithographic technology.

Now, with the same angular and material constraint we will design a new BO Fresnel wedge for  $0.35 \mu\text{m}$  in the UV. Repeating the above procedure just illustrated we find the subprism height  $h = 0.7 \mu\text{m}$ , the base of each subprism (and grating period) to be  $d = 1.15 \mu\text{m}$ , the binary step width  $w \approx 0.072 \mu\text{m}$ , and the binary step height  $h \approx 0.044 \mu\text{m}$ . This design is beyond the current or even near term projected technology. A further examination is required.

In both cases, i.e. the IR and UV designs, the value of  $m \approx 1.13$ , but what is the meaning of non-integer values of  $m$ ? From Fig. 4 we saw that for small exit angles and high indices of refraction, the value of  $m$  does approach an integer 1. However, for low index materials that are used at higher exit angles,  $m$  is not an integer.

## 6. UTILIZING A FRAUNHOFER APPROACH TO DEVELOP AN ALTERNATE APPROXIMATION OF A FRESNEL WEDGE

As discussed previously, we will take an approach, the Fraunhofer approximation in particular, as described by

Goodman<sup>6</sup>. The results here are slightly different from the scalar approximation presented earlier. These results provide insight into the significance of the non-integer values of  $m$  that may result in energy being displaced from the desired order to undesired ones.

Let's assume that light composed of planar wave fronts strikes the grating structure, i.e. the triangular ridges shown in Fig. 3, internally from the left, and although a small fraction of the light that illuminates each ridge is reflected, the bulk is transmitted on through in accordance with Snell's law as given in Eq (1). Although the refracted beams *emerge* from the grating initially parallel to each other, diffraction takes over and the transmitted light is very noticeably ordered into regions of high and low intensity. In order to determine the resulting diffraction pattern in the far field we use the approach of Goodman<sup>6</sup> and consider the grating as a phase transformation of the light passing through it. From there on, the spatially modulated wavefronts diffract as they propagate.

The details of the phase transformation and subsequent Fraunhofer derivation will be presented in a later paper, and we find the intensity distribution to be estimated by

$$I(y) = I_0 \text{sinc}^2 \left( \frac{y + (n_1 - n_2) \frac{h}{d} z}{\frac{\lambda z}{d}} \right) \left( 1 + 4 \sum_{p=1}^{\frac{P-1}{2}} \cos \left( 2\pi p \frac{d}{\lambda z} y \right) + 4 \left[ \sum_{p=1}^{\frac{P-1}{2}} \cos \left( 2\pi p \frac{d}{\lambda z} y \right) \right]^2 \right), \quad (11)$$

where  $I_0$  is a combination of parameters that is given by

$$I_0 = I_0(x) = C \left( \frac{dLT}{\lambda z} \right)^2 \text{sinc}^2 \left( \frac{x}{\frac{\lambda z}{L}} \right). \quad (12)$$

In the diffraction pattern represented by Eqs(11) and (12),  $C$  contains all the electromagnetic constants required in going from complex field amplitude to a real, time-averaged intensity,  $z$  = the axial distance from the plane containing the grating to the plane of observation,  $L$  = the length of the grating in the  $x$  direction, i.e. normal to the plane of Fig. 3,  $T$  = amplitude transmittance through both the front and back surfaces of the grating,  $P$  = the number of grating periods (assumed to be an odd integer  $> 3$  for this derivation), and  $p$  = a summation index.

Examination of Eq (11) shows that aside from  $I_0$ , which contains only constants and the less important  $x$  dependence, it consists of two key terms. The cosinusoidal function to the right of the  $\text{sinc}^2$  function is in essence an intensity interference pattern due to  $P$  line sources that are spaced a distance  $d$  apart. The interaction between them will result in major constructive interference peaks wherever  $yd/\lambda z$  = a positive or negative integer, including 0, and  $P-2$  minor constructive interference peaks that are spaced uniformly between them. The leftmost portion of Eq (11), the  $\text{sinc}^2$  function, is the Fraunhofer diffraction pattern due to a single rectangular slit of width  $d$ , but whose peak,  $y_{\text{sinc max}}$ , has been shifted down from the optical axis at  $y = 0$  to the position  $y_{\text{sinc max}} = -(n_1 - n_2)hz/d$ . The zeros of the  $\text{sinc}^2$  function occur wherever  $y = y_{\text{sinc max}} \pm m(\lambda z/d)$ , where  $m$  too equals a positive or negative integer, but not at  $m = 0$ .

What this means for the net diffraction pattern that results is that if  $y_{\text{sinc max}}$  coincides with one of the major constructive interference peaks, which are located at  $y = m' \lambda z/d$  with  $m' = 0, \pm 1, \pm 2, \dots$ , then only that *interference order* will be unattenuated. The zeros of the  $\text{sinc}^2$  function will coincide exactly with all the other major interference peaks, thus preventing their formation, and only the minor interference peaks will be passed, although strongly suppressed, by the subpeaks of the  $\text{sinc}^2$  function, which decay rapidly away from the strong peak located at  $y_{\text{sinc max}}$ . This, then, is the ideal behavior of a Fresnel wedge. This ideal *filtering* behavior only occurs when the height of each subprism  $h = q\lambda/(n_1 - n_2)$ , i.e. Eq (6) with  $n_2 = 1$ .

If this condition on  $h$  is not met, then the  $\text{sinc}^2$  function will be shifted from its ideal position with respect to the

major and minor interference peaks due to the P line sources. It's filtering behavior will be less than ideal, resulting in the desired order being attenuated and substantially reduced suppression of the undesired orders. Figures 6 and 7 shows plots of Eq. (11) calculated for  $h = 3 \lambda / (n_1 - 1)$  and  $h = 2.95 \lambda / (n_1 - 1)$ . Compare Fig. 7 to Fig. 8, which shows the experimental results of a Fresnel wedge that was made and measured at the Naval Weapons Center, China Lake, Ca. last year. The height,  $h$ , of the subprisms on this Fresnel wedge does not meet the requirements of Eq. (6). The authors hope to have a Fresnel wedge that satisfies this restriction for measurements in the very near future.

## 7. CONCLUSION

It has been shown that when designing BO elements, it may be important to look judiciously at not only the design methodology, but the manufacturability. Fraunhofer analysis of the Fresnel wedge indicates that it is important to adhere to diffraction constraints when designing BO elements. While the assumptions and constraints in Section 5 were used to more closely approximate a region of a Fresnel type lens which may be utilized at a variety of angle around the design exitance angle  $\Theta$ , other models<sup>7</sup> are certainly more accurate for Fresnel wedges utilized at such large angles. Hence, it appears that the efficiency of an element is governed not only by the manufacturing process, but also by the material properties of various regions of the optical element. Anti-reflection coatings may utilized on the surfaces of elements that do not contain BO structures to reduce Fresnel reflected losses; however, it may not be possible to use them on the surfaces containing BO structures since overcoated structures act as waveguides producing side bands, or spurious orders. It also appears that the choice of substrate material may play a role in the amplitude of side bands or ghosting. With the proper choice of material (hence  $n$  the index of refraction) and  $q$ , one may be able to control these unwanted effects.

## 8. REFERENCES

1. W.C. Sweatt, "Describing Holographic Optical Elements as Lenses," J. Opt. Soc. Am. 67,803(1977).
2. W.A. Kleinhans, "Aberrations of Curved Zone Plates and Fresnel Lenses," Appl. Opt. 16, 1701(1977)
3. G.J. Swanson, "Binary Optics Technology: The Theory and Design of Multi-level Diffractive Optical Elements," Technical Report 854, MIT Lincoln Laboratory, 14 August 1989
4. W.H. Southwell, "Binary Optics from a Ray Tracing Point of View," Technical Digest on Lens Design, 1990 (Optical Society of America, Washington, D.C., 1990) Vol.10, pp.13-14
5. L.F. DeSandre, "Extinction Theorem Analysis of Diffraction Anomalies in Overcoated Gratings," Ph.D. Thesis, Optical Sciences Center, University of Arizona, 1989
6. J.W. Goodman, Introduction to Fourier Optics, ch 4-5, McGraw-Hill, San Francisco, Ca., 1968
7. M. Elson and L. DeSandre, Private Communication, Naval Weapons Center, Ca., 1991



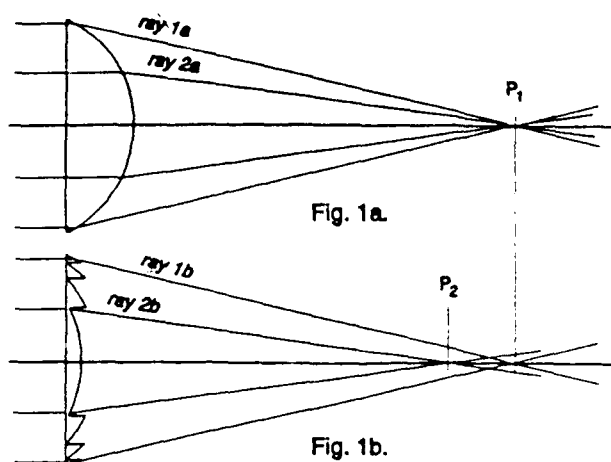


Fig. 1a. A classical thick lens aspherized for minimum spherical aberration. Both rays 1a and 2a cross the optical axis at the point P<sub>1</sub>. In Fig. 1b. the Fresnel equivalent lens is shown. While ray 1b crosses the axis at point P<sub>1</sub>, ray 2b crosses the optical axis at point P<sub>2</sub>. This is due to the fact that the edge of the medial section ray 2b was simply collapsed in forming the Fresnel lens equivalent.

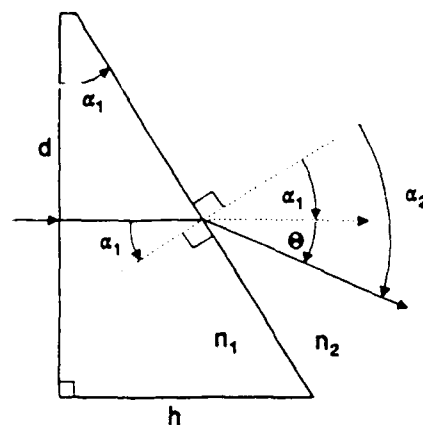


Fig. 2. Shown is a right triangular prism with an index of refraction  $n_1$  and prism angle  $\alpha_1$ . Light enters the prism perpendicular to the front surface and strikes the back surface at angle  $\alpha_1$ . From Snell's law,  $n_1 \sin \alpha_1 = n_2 \sin \alpha_2$ , light exits the prism at angle  $\alpha_2$ . The exitance media has an index of refraction  $n_2$ .

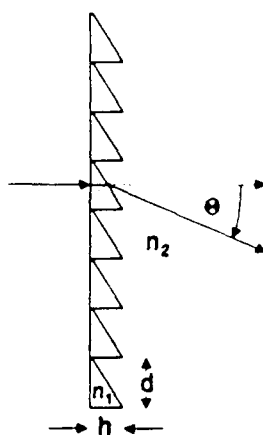


Fig. 3. The Fresnel wedge has an index of refraction  $n_1$ , the height of each subprism is  $h$ , and the grating period is  $d$ . Light is incident onto the grating perpendicular to the front surface, and the design exitance angle is  $\theta$ . The exitance media has an index of refraction  $n_2$ .

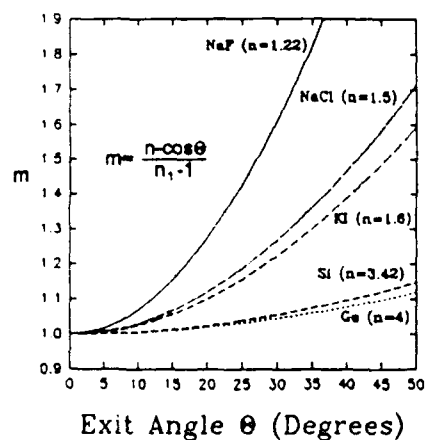


Fig. 4. Shown is a plot of grating order versus exitance angle  $\theta$  for a variety of materials for a Fresnel wedge with the constraints presented.

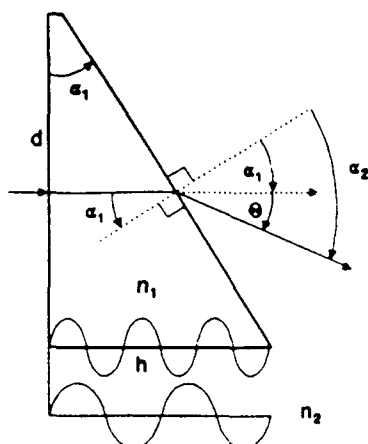


Fig. 5. The right triangular prism shown here is similar to that in Fig. 2, but with the height  $h = \lambda/(n_1-1)$ . Light traveling in air is shown to be in phase with the light traveling just within the prism's edge.

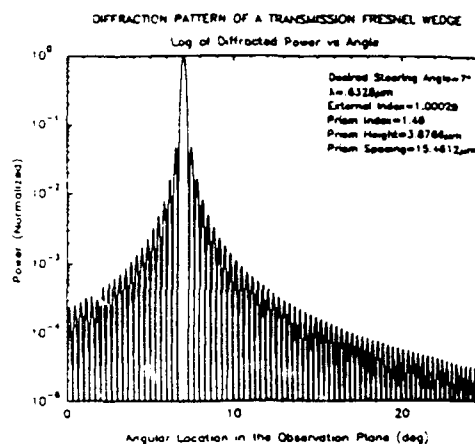


Fig. 6. Shown is a plot of what the normalized Fraunhofer diffraction pattern of a Fresnel wedge versus angular location in the observation plane might look like for  $h = 3\lambda/(n_1-1)$ .

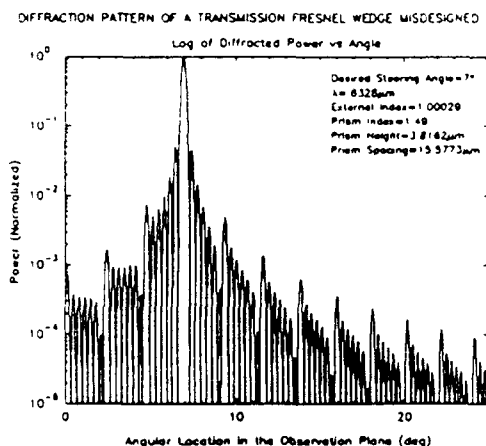


Fig. 7. Shown is a plot of what the normalized Fraunhofer diffraction pattern of a Fresnel wedge versus angular location in the observation plane might look like for  $h = 2.95\lambda/(n_1-1)$ .

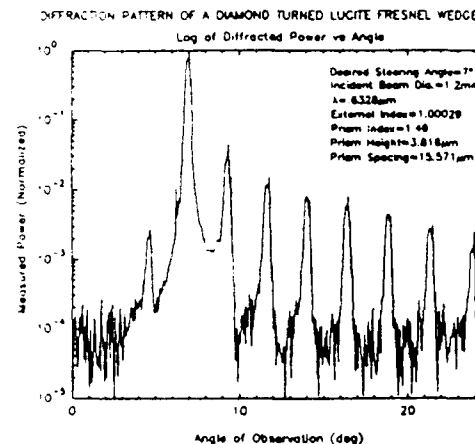


Fig. 8. Shown is a plot of the measured and normalized Fraunhofer diffraction pattern of a Lucite Fresnel wedge versus observation angle that was constructed using  $h \approx 2.95\lambda/(n_1-1)$ . The refractive index of Lucite is 1.49, and the design and measurement wavelength used was 632.8 nm.